Synthesis, Mass Spectrometry, and Spectroscopic Properties of a Dinuclear Ruthenium Complex Comprising a 20 Å Long Fully Aromatic Bridging Ligand

Eléna Ishow,[†] André Gourdon,*[,†] Jean-Pierre Launay,[†] Claudio Chiorboli,*[,‡] and Franco Scandola[‡]

Groupe Electronique Moléculaire, CEMES-CNRS UPR 8011, BP 4347, 29 Rue Jeanne Marvig, 31055 Toulouse, France, and Dipartimento di Chimica, Centro di Reattività e Catalisi CNR, Università di Ferrara, Via L. Borsari 46, 44100 Ferrara, Italy

Received October 15, 1998

The luminescent dinuclear ruthenium complex $[(bpy)_2Ru(bqpy)Ru(bpy)_2]^{4+}$ (**1**) comprising the 20 Å long fully aromatic bridging ligand bqpy has been synthesized by successive reactions from suitable precursor complexes. Investigations in electrospray mass spectrometry and ^1H NMR spectroscopy have indicated the formation of supramolecular aggregates by strong π-stacking of the large aromatic parts. Despite the extended aromatic character of the bqpy bridging ligand, electrochemical and spectroscopic studies of the dinuclear complex have shown that the complex is composed of four noninteracting parts: two $Ru(bpy)_3^{2+}$-type units bridged by two bqpy-localized fragments similar to two fused phenazine moieties.

Introduction

Oligonuclear polypyridyl Ru(II) complexes are currently being much investigated because of their rich electrochemical and photochemical properties which render them very attractive systems for modeling long-range electron and energy transfer,[1] known to play a crucial role in numerous biological processes (respiration chain, photosynthesis, DNA oxidative cleavage).[2] Most of the systems described so far comprise a bridging ligand in which π-conjugated monomeric units are linked by σ bonds. Possible rotation around these σ bonds is then allowed which causes loss of coplanarity of the π electrons or aromatic parts and consequently a decrease of the long-distance electronic coupling between the terminal sites. Therefore, long, planar, rigid polyaromatic bridges are very convenient as building blocks for the construction of polynuclear metal complexes. They are expected to provide relatively strong intercomponent electronic coupling, and thus to behave as good and well-defined connectors for long-range energy and/or electron-transfer processes in an optimized and known geometry.

For this reason, we have recently studied[3] polynuclear complexes bridged by fully rigid polyaromatic ligands such as the tetrapyrido[3,2-*a*:2′,3′-*c*:3″,2″-*h*:2‴,3‴-*j*]phenazine (tpphz).

The very low solubility of these long polyaromatic ligands, due to strong $\pi-\pi$ interactions, can impede their synthesis and

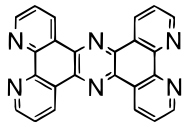

tpphz

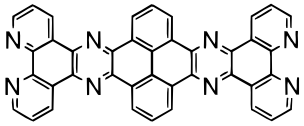

bqpy

the preparation of their complexes. However we have recently shown that corresponding transition metal complexes of varied geometry and metal centers can be synthesized following a building-block stepwise construction of the bridging ligand onto a well-soluble ruthenium complex precursor.[3,4] As the bridging ligands exhibit an extended aromatic character, such a $\pi-\pi$ aggregation behavior is expected to be retained within the complexes when the steric and/or the Coulombic repulsions are strongly counterbalanced by the favorable van der Waals interactions involved in $\pi-\pi$ stacked systems. For instance, the dimerization in solution of the monomolecular complex $[(bpy)_2Ru(tpphz)]^{2+}$ was clearly evidenced through the dramatic changes of the NMR spectrum upon temperature and concentration variations. This dimerization by $\pi-\pi$ stacking of the tpphz part was not observed for the dinuclear complex $[(bpy)_2Ru$-

* To whom correspondence should be addressed. For A.G.: fax, +33 (0)5 62 257 999; e-mail, gourdon@cemes.fr. For C.C.: fax, +39 (0)532 240 709; e-mail, chc@dns.unife.it.

† CEMES.

‡ Università di Ferrara.

(1) (a) Collin, J.-P.; Gavina, P.; Heitz, P.; Sauvage, J.-P. *Eur. J. Inorg. Chem.* **1998**, *1*, 1. (b) Barigelletti, F.; Flamigni, L.; Collin, J.-P.; Sauvage, J.-P. *Chem. Commun.* **1997**, 333. (c) Livoreil, A.; Sauvage, J.-P.; Armaroli, N.; Balzani, V.; Flamigni, L.; Ventura, B. *J. Am. Chem. Soc.* **1997**, *119*, 12114. (d) Balzani, V.; Juris, A.; Venturi, M.; Campagna, S.; Serroni, S. *Chem. Rev.* **1996**, *96*, 759. (e) Sauvage, J.-P.; Collin, J.-P.; Chambron, J.-C.; Guillerez, S.; Coudret, C.; Balzani, V.; Barigelletti, F.; DeCola, L.; Flamigni, L. *Chem. Rev.* **1994**, *94*, 993.

(2) Holmlin, R. E.; Dnadliker, P. J.; Barton, J. K. *Angew. Chem., Int. Ed. Engl.* **1997**, *36*, 2714.

(3) (a) Bolger, J.; Gourdon, A.; Ishow, E.; Launay, J.-P. *Inorg. Chem.* **1996**, 35, 2937. (b) Bolger, J.; Gourdon, A.; Ishow, E.; Launay, J.-P. *J. Chem. Soc. Chem. Commun.* **1995**, 1799. (c) Ishow, E.; Gourdon, A.; Launay, J.-P.; Lecante, P.; Verelst, M.; Chiorboli, C.; Scandola, F.; Bignozzi, C.-A. *Inorg. Chem.* **1998**, *37*, 3603. (d) Ishow, E.; Gourdon, A.; Launay, J.-P. *Chem. Commun.* **1998**, 1909.

(4) (a) Reek, J. N.; Schenning, A. P.; Bosman, A. W.; Meijer, E. W.; Crossley, M. J. *Chem. Commun.* **1998**, 11. (b) Bodige, S.; MacDonnell, F. M. *Tetrahedron. Lett.* **1997**, *38*, 8159. (c) MacDonnell, F. M.; Bodige, S. *Inorg. Chem.* **1996**, *35*, 5758. (d) Wärnmark, K.; Thomas, J.; Heyke, O. Lehn, J.-M. *J. Chem. Soc., Chem. Commun.* **1996**, 701.

10.1021/ic9812196 CCC: $18.00
Published on Web 03/12/1999

Scheme 1. Synthesis of the Complex 1[a]

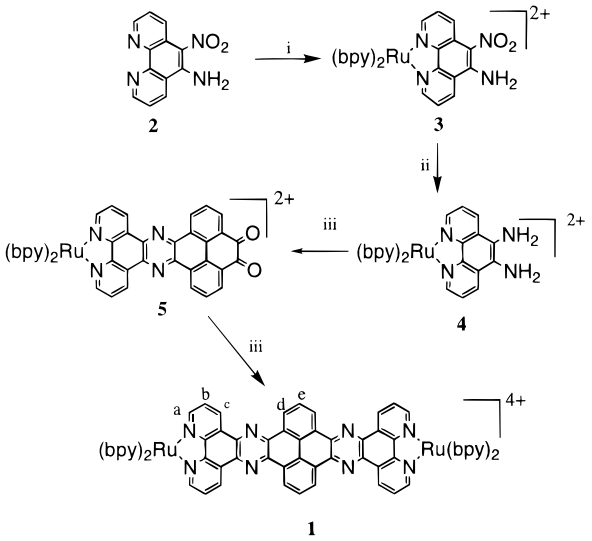

[a] Reagents: (i) $[Ru(bpy)_2Cl_2]$; (ii) $NH_2NH_2 \cdot H_2O$, Pd/C 10%; (iii) tetraketopyrene.

$(tpphz)Ru(bpy)_2]^{4+}$. Indeed, the relatively short intermolecular Ru−Ru distance (12.77 Å determined by X-ray diffraction), precludes an efficient packing. Calculations have shown that, with parallel tpphz quinoxaline planes at an interplane distance of 3.5 Å and the Ru−Ru axes in a perpendicular conformation, the $Ru(bpy)_2$ extremities are at van der Waals contact with intermolecular Ru−Ru distances below 10 Å. At this distance the Coulombic repulsions between the metallic moieties are probably too high if compared to the attractive van der Waals forces, which prohibits the formation of stable $\pi-\pi$ dimer. It can be presumed that significantly larger intermetallic distances would considerably reduce the intermolecular electrostatic repulsions between each 4^+ charged complex and would then enable a more efficient $\pi-\pi$ stacking of two dinuclear complexes. Along these lines, we have synthesized[3d] the dinuclear complex **1** of bis-{dipyrido[3,2-*f*:2′,3′-*h*]quinoxalo}-[2,3-*e*:2′,3′-*l*]pyrene (bqpy) shown in Scheme 1 in which the calculated intermetallic distance is ca. 20 Å, long enough to allow an efficient supramolecular aggregation.

Experimental Section

General Procedures. Starting materials were either prepared according to literature procedures or purchased from Aldrich, Fluka, or Acros and used without further purifications. Solvents were used as received except DMF (for electrochemical measurements) which was purified according to reference.[5] Chromatographic purifications on column and preparative plates were respectively carried out on silica gel 60 (70−230 mesh) and on 2 mm-thick silica gel plates. ^1H NMR spectra were recorded with Bruker WF-250, Bruker AMX-400 spectrometers (250 and 400 MHz, respectively) (CD_3CN at $\delta = 1.95$ ppm as internal standard); the spectra were processed with the programs SwaN-MR[6] or Mestre-C.[7] FABMS were obtained on a Nermag R10-R10 spectrometer (3-nitrobenzyl alcohol as a matrix; 8 keV); ESMS were measured on a Perkin-Elmer SCIEX spectrometer equipped with a LCMS System API 100 (60−120 eV). UV/visible spectra were recorded on a Shimadzu UV-3100 spectrophotometer. Electrochemical measurements were performed on an Electromat 2000. Cyclic voltammograms were obtained using a platinum working electrode, a platinum auxiliary electrode and a saturated potassium chloride calomel reference electrode (Tacussel). Linear and differential pulsed voltammetry were done using a platinum rotating disk electrode. At the end of each experiment, ferrocene was added as an internal standard with $E_{1/2}(Fc^+/Fc) = 0.48$ V vs SCE. The potentials were then automatically corrected for uncompensated cell resistance. Steady-state luminescence studies were performed using a Perkin-Elmer MPF 44E spectrofluorimeter. For 77 K emission spectra, an Oxford DN704 cryostat equipped with an Oxford DTC-2 temperature controller was used. The reported spectra are corrected for the detector response. Emission lifetimes were measured using a PRA system 3000 time-correlated single photon counting apparatus equipped with a Norland model 5000 MCA card, and a hydrogen discharge pulsing lamp (50 kHz, half-width 2 ns). The decays were analyzed by means of Edinburgh FLA900 software. Alternatively, an Applied Photophysics laser flash photolysis apparatus was used using a Continuum model Surelite II Nd:YAG laser (half-width 4−6 ns), frequency doubled (532 nm, 330 mJ) or tripled (355 nm, 160 mJ). The photomultiplier (Hamamatsu R928) signal were processed by means of a LeCroy 9360 (600 MHz, 5 Gs/s) digital oscilloscope.

Luminescence quantum yields were measured in optically diluted solutions, using $[Ru(bpy)_3]^{2+}$ in oxygen-free acetonitrile ($\Phi = 0.06$) as reference emitter. Estimated experimental errors in the reported data are as follows: absorption and emission maxima, ±2 nm; emission lifetimes and emission quantum yields, ±10%.

Synthesis of {[Ru(bpy)$_2$(2)](PF$_6$)$_2$·H$_2$O} (3). A suspension of $Ru(bpy)_2Cl_2 \cdot 2H_2O$ (271 mg, 0.52 mmol) and 5-amino-6-nitro-1,10-phenanthroline (**2**)[3a] (150 mg, 0.62 mmol) in deoxygenated ethanol (40 mL) was stirred for 4 h under reflux. After cooling at room temperature and filtration, the deep orange solution was diluted with toluene (60 mL) and concentrated under vacuum until an orange solid precipitated. The collected solid was then subjected to chromatographic purification on silica gel column. Pure acetonitrile was used as first eluent till stabilization of an orange band and then replaced by a salted acetonitrile solution with increasing NH_4PF_6 concentration (final concentration: 0.5 g L^{-1}). After removal of a first yellow fraction, the bright-orange band was collected and concentrated at the rotary evaporator. The complex was then redissolved in CH_2Cl_2 and filtrated to remove excess salt; methanol and toluene were eventually added to the solution and concentrated as previously till full precipitation of pure nitro-amino ruthenium complex. Yield: 420 mg (82%). ^1H NMR (CD_3CN): δ 7.38−7.31 (m, 3 H, H5′-H5″-H5‴), 7.44 (ddd, $J = 1.2$, 5.7, 8.2 Hz; 1 H, H5), 7.67 (dd, $J = 5.2$, 8.8 Hz; 1 H, Hb′), 7.82 (dd, $J = 5.3$, 8.4 Hz; 1 H, Hb), 7.84 (dd, $J = 1.1$, 5.2 Hz, 1 H, Ha′), 8.07 (dd, $J = 1.4$, 8.1 Hz; 2 H, H4′-H4‴), 8.14 (dd, $J = 1.4$, 7.9 Hz; 2 H, H4−H4″), 8.24 (dd, $J = 1.1$, 5.3 Hz; 1 H, Ha), 8.44 (s, 2 H, NH_2), 8.56 (d, $J = 7.6$ Hz, 2 H, H3′-H3‴), 8.59 (d, $J = 7.6$ Hz, 2 H, H3−H3″), 9.04 (dd, $J = 1.1$, 8.8 Hz, 1 H, Hc′), 9.26 (dd, $J = 1.1$, 8.4 Hz; 1 H, Hc). FABMS (8 keV) *m*/*z*: 799 $[M - PF_6^-]^+$, 653 $[M - 2PF_6^- + H]^+$. Anal. Calcd for $C_{32}H_{24}N_8O_2RuP_2F_{12} \cdot H_2O$ (961.6): C, 40.0; H, 2.7; N, 11.70. Found C, 40.25; H, 3.00; N, 11.27.

Synthesis of {[Ru(bpy)$_2$(5,6-diamino-1,10-phenanthroline)](PF$_6$)$_2$·2H$_2$O} (4). To a saturated and refluxing solution of **3** (200 mg, 0.21 mmol) in a 1/1 methanol and ethanol mixture was added Pd/C (10%) (72 mg). After 5 min, hydrazine monohydrate (55%; 120 mL; 2.1 mmol) was added rapidly to the refluxing mixture. The reaction was followed by thin-layer chromatography (SiO_2: NH_4PF_6/acetonitrile) and gave within 5 min after the hydrazine addition a slightly more red and polar product corresponding to the diamino complex. Another portion of hydrazine was added after 30 min, and the mixture was subsequently heated for 30 min. The solution was then filtrated through Celite. The bright red filtrate was diluted with toluene. Concentration under reduced pressure with a rotary evaporator (the water bath temperature must be kept below 30 °C to avoid any irreversible degradation) led to the precipitation of a red solid. The pure complex was collected by filtration and dried under vacuum. Yield: 172.5 mg (89%). ^1H NMR (CD_3CN): δ 4.78 (s, 4 H, NH_2), 7.21 (ddd, $J = 1.4$, 5.8, 7.4 Hz, 2 H, H5′), 7.45 (ddd, $J = 1.4$, 5.8, 7.4 Hz; 2 H, H5), 7.54. (ddd, $J = 0.7$, 1.4, 6.1 Hz; 2 H, H6′), 7.74 (dd, $J = 5.1$, 8.6 Hz; 2 H, Hb), 7.84 (dd, $J = 1.1$, 5.1 Hz; 2 H, Ha), 7.86 (ddd, 2 H, $J = 0.7$, 1.4, 6.4 Hz; H 6), 8.07 (ddd, *J*

(5) Fees, J.; Kaim, W.; Moscherosch, M.; Matheis, W.; Klima, J.; Krejcik, M.; Zalis, S. *Inorg. Chem.* **1993**, *32*, 166.
(6) Balacco, G. *J. Chem. Inf. Comput. Sci.* **1994**, *34*, 1235.
(7) MestRe C 1.5.1, a freeware program for NMR data processing. Cobas, J. C.; Cruces, J.; Sardina, F. J. http://qobrue.usc.es/jsgroup/MestRe-C/MestRe-C.html.

= 1.4, 7.7, 8.1 Hz; 2 H, H4′), 8.10 (ddd, J = 1.4, 7.7, 8.1 Hz; 2 H, H4), 8.50 (d, J = 9.3 Hz, 2 H, H3′), 8.52 (dd, J = 1.1, 8.6 Hz; 1 H, Hc), 8.55 (d, J = 9.1 Hz, 2 H, H3). FABMS (8 keV) *m/z*: 769 [M − PF_6^- + H]$^+$, 623 [M − 2PF6$^-$ + H]$^+$. Anal. Calcd for $C_{32}H_{26}F_{12}N_8P_2Ru\cdot 2H_2O$ (931.1): C, 40.5; H, 3.2; N, 11.8. Found: C, 40.6; H, 3.0; N, 12.0.

Synthesis of {(bpy)$_2$Ru(bqpy)Ru(bpy)$_2$](PF$_6$)$_4$·8H$_2$O} (1). A 2.2 equiv amount of **4** (50 mg, 0.055 mmol) and 1 equiv of tetraketopyrene were dissolved in a acetonitrile/water/acetic acid mixture (20 mL/15 mL/ 1 mL). The solution was then deoxygenated before heating at 75 °C during 4 days. After cooling at room temperature and addition of toluene, the solution was concentrated with a rotary evaporator until precipitation of a red solid. The solid was recuperated by filtration, washed with ethanol and water, and purified by two chromatographies on silica gel. The product was first subjected to a column chromatography using as eluent a salt gradient of NH_4PF_6 in acetonitrile (final concentration: 0.32 g.L^{-1}). The red UV-luminescent fractions were regrouped, evaporated, and redissolved in a water/acetonitrile mixture to remove the salt excess. After concentration and precipitation of a red solid in the aqueous layer, the solid was collected by filtration. A second chromatography purification was carried out using this time SiO_2 preparative plates and as eluent a salted solvent mixture (acetonitrile/water/NH_4PF_6: 200 mL/10 mL/450 mg) and allowed complete separation from the mononuclear complex **5** (see Supporting Information for further experimental details). After elution, the red UV-luminescent band was scratched; the silica gel was then crushed and thoroughly washed on a frit by a solution of NH_4PF_6 in acetonitrile. The pure red complex was finally isolated by addition of water, concentration under vacuum, filtration, and drying under vacuum. Yield: 32 mg (64%). ^{1}H NMR (250 MHz, CD_3CN, 298 K, 2.6 × 10^{-4} mol L^{-1}): δ 7.21 (ddd, J = 6.2, 6.2, 1.2 Hz; 4 H; H5′), 7.52 (ddd, J = 1.2, 6.5, 6.5 Hz; 4 H; H5), 7.82 (d, J = 5.3 Hz, 4 H; H6′), 7.92 (d, J = 5.1 Hz, 4 H, H6), 7.99 (dd, J = 5.3, 8.2 Hz, 4H, Hb), 8.06 (ddd, J = 1.4, 7.9, 8.0 Hz, 4 H, H4′), 8.17 (ddd, J = 1.4, 7.9, 8.0 Hz, 4 H, H4), 8.30 (dd, J = 1.3, 5.4, Hz, 4 H, Ha); 8.38 (d, J = 7.0 Hz, 2 H, He), 8.57 (d, J = 8.5 Hz, 4 H, H3′), 8.61 (d, J = 8.3 Hz, 4 H, H3), 9.63 (d, J = 8.2 Hz, 4 H, Hc), 9.74 (d, J = 7.0 Hz, 4 H, Hd). UV−vis (acetonitrile): λ_{max} nm (ϵ × 10^{-3} mol L^{-1} cm^{-1}) = 421 (48), 332 (66), 287 (139). MS (ESMS, solvent: CH_3CN/H_2O (1/1 v/v), injection 5 mL min^{-1}) *m/z*: 1873 [M − PF_6^-]$^+$, 864 [M − 2PF_6^-]$^{2+}$, 526 [M − 3PF_6^-]$^{3+}$, 359.9 [M − 4PF_6^-]$^{4+}$. Anal. Calcd for $C_{80}H_{50}N_{16}Ru_2P_4F_{24}\cdot 8H_2O$: C, 41.26; H, 3.03; N, 12.03. Found: C, 40.59; H, 3.00; N, 12.00.

Calculations. The energy-minimized structure of the free ligands bqpy and tpphz was calculated using the semiempirical method AM1.[8] The geometry of the binuclear complex was obtained by molecular mechanics with the program Cerius2 (Biosym/Molecular Simulations)[9] using the Universal Force Field.[10] Parametrization of the Ru−N distances was done using the X-ray structures of the CSSR database[11] containing the Ru(bpy) fragment. The value Ru−N(pyridine) = 2.05 Å was used with an harmonic potential function and force constants k = 300 (kcal/mol) Å^2. Calculations of the electronic structures were then performed with the extended Hückel approximation using the CACAO program.[12]

Results and Discussion

Synthesis. As expected, the direct synthesis of the polyquinoxalinic bridging ligand bqpy encountered serious insolubility problems related to extensive $\pi-\pi$ intermolecular interactions of such a large polyaromatic skeleton. Only mixtures of insoluble products resulted from reaction of 5,6-diamino-1,10-phenanthroline and tetraketopyrene. To overcome these insolubility limitations, we have adopted a building-block stepwise construction of the bqpy ligand onto a well-soluble ruthenium complex precursor shown in Scheme 1.

Attempts to prepare the precursor diamino complex **4** by reaction of 5,6-diamino-1,10-phenanthroline[3a] with [Ru(bpy)$_2$Cl$_2$] in the presence of $AgCF_3SO_3$ mostly gave a phenanthrolinediimido complex and the dinuclear [(bpy)$_2$Ru(tpphz)Ru(bpy)$_2$]$^{4+}$ arising from the auto-condensation of the phendiamine in oxidizing conditions. In contrast, the nitro-amino precursor **3** has been cleanly obtained in 82% yield by reacting 5-amino-6-nitro-1,10-phenanthroline[3] **2** and [Ru(bpy)$_2$Cl$_2$] in refluxing ethanol for 3 h. Subsequent reduction of the nitro group by hydrazine hydrate on 10% Pd/C furnished in high yield (89%) the pure diamino complex **4**. This latter was finally allowed to react with tetraketopyrene[13] in a refluxing aqueous acetonitrile/acetic acid mixture for 4 d and gave the dinuclear ruthenium complex [(bpy)$_2$Ru(bqpy)Ru(bpy)$_2$]$^{4+}$ **1** in 64% yield after chromatographic purifications. Acetic acid catalysis and prolonged heating seem here to be essential for full completion of the 2-fold condensation. Isolation and characterization by NMR spectroscopy and electrospray mass spectrometry of the stable monocondensation intermediate product **5** (details in Supporting Information) after few hours reflux have actually shown the double-step character of the whole condensation.

^{1}H NMR. All compounds were characterized by ^{1}H and ^{1}H−^{1}H COSY NMR spectroscopy. As expected on the basis of our previous results on shorter di- and tetranuclear[3] tpphz ruthenium complexes and contrary to most short ruthenium-bipyridyl multinuclear complexes for which full ^{1}H NMR characterization requires enantiomeric resolutions, the proton NMR signals of complex **1** were unambiguously assigned. This simple magnetic pattern (Figure 1) actually originates from the large separation between the two ruthenium centers (ca. 20 Å). At such distances, each chiral center is not influenced by its neighbors, so that the ^{1}H NMR spectra of all stereoisomers exactly superimpose.

As observed for monometallic complexes comprising a large polyaromatic part,[3,14,15] strong dependence on concentration was observed for the dinuclear complex. On increasing the concentration and keeping the same relaxation time scale, the resonance signals of the quinoxalinic protons and more particularly those of the pyrene protons Hd and He dramatically broaden and are downfield shifted up to 0.9 ppm. Conversely, the ancillary bipyridine protons are less affected and their chemical shifts only slightly move upfield (0.1 ppm). The displacements of some proton signals while varying concentration or temperature are attributed to $\pi-\pi$ stacking of the aromatic bridging ligands. Upon intra- or intermolecular aggregation of aromatic molecules, changes in the electronic density occur and generate novel cycle current effects[16] hence the observed chemical shift displacements. The significant broadness for such noncovalent systems

(8) Dewar, M. J. S.; Zoebisch, E. G.; Healy, E. F.; Stewart, J. J. P. *J. Am. Chem. Soc.* **1985**, *107*, 3902.
(9) *CERIUS*^{2} *Molecular Simulation Program*; Molecular Simulations Inc.: San Diego, CA.
(10) (a) Rappé, A. K.; Casewit, C. J.; Colwell, K. S.; Goddard, W. A.; Skiff, W. M. *J. Am. Chem. Soc.* **1992**, *114*, 10024. (b) Rappé, A. K.; Colwell, K. S.; Casewit, C. J. *Inorg. Chem.* **1993**, *32*, 3438.
(11) Allen, F. H.; Davies, J. E.; Galloy, J. J.; Johnson, D.; Kennard, O.; Macrae, C. F.; Mitchell, E.; Smith, J. M.; Watson, D. G. *J. Chem. Inf. Comput. Sci.* **1991**, *31*, 187.
(12) CACAO Program (Computer Aided Composition of Atomic Orbitals). Mealli, C.; Proserpio, D. M. *J. Chem. Educ.* **1990**, *67*, 399.
(13) Vollmann, H.; Becker, H.; Corell M.; Streeck, H. *Justus Liebigs Anal. Chem.* 1937, **531**, 2.
(14) Rudi, A.; Kashman, Y.; Gut, D.; Lellouche, F.; Kol, M. *J. Chem. Soc., Chem. Commun.* **1997**, 17.
(15) Gourdon, A.; Launay, J.-P. *Inorg. Chem.* **1998**, *37*, 5336.
(16) See for instance: (a) Anderson, H. *Inorg. Chem.* **1994**, *33*, 972. (b) Hunter, C. A.; Sanders, J. K. *J. Am. Chem. Soc.* **1990**, *112*, 5525. (c) Philp, P.; Stoddart, J. F. *Angew. Chem., Int. Ed. Engl.* **1996**, *35*, 1154. (d) Whitlock, B. J.; Whitlock, H. W. *J. Am. Chem. Soc.* **1990**, *112*, 3910. (e) Ashton, P. R.; Ballardini, R.; Balzani, V.; Credi, A.; Gandolfi, M. T.; Menzer, S.; Pérez-Garcia, L.; Prodi, L.; Stoddart, J. F.; Venturi, M.; White, A. J. P.; Williams, D. J. *J. Am. Chem. Soc.* **1997**, *117*, 11171.

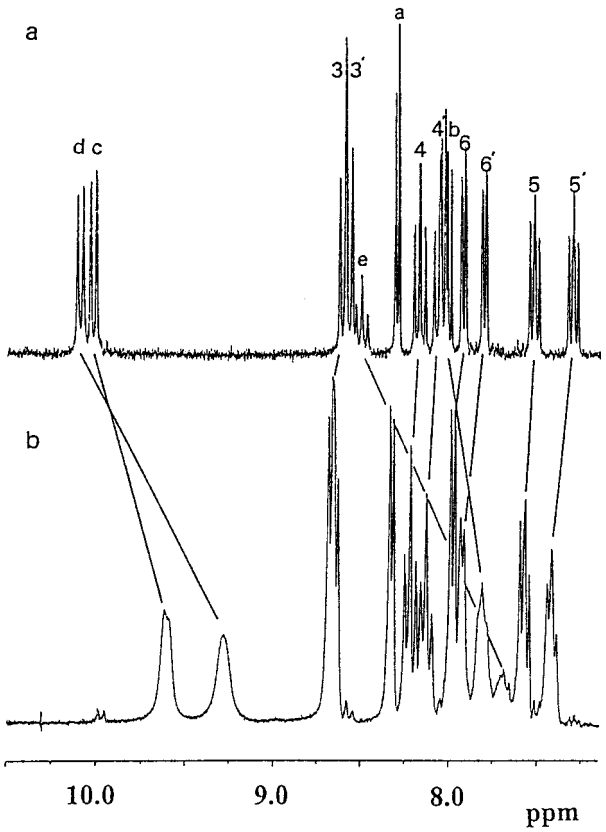

Figure 1. ^{1}H NMR spectra of **1** at concentrations (a) 2.5×10^{-4} and (b) 1.5×10^{-3} mol L^{-1}. The attribution refers to the labeling in Scheme 1.

relying on $\pi-\pi$ interactions or pure hydrogen bonding must considerably reduce the freedom degrees of the protons and increase their relaxation time. Unfortunately, NOESY experiments performed in concentrated solutions failed for detecting intermolecular resonance transfer between the pyrene and the bpy H5 and H6 protons probably because of the high molecular weight range and, above all, possible translationnal motions within the dimer. The first association constant monomer−dimer can be calculated at low concentration (below 1.9×10^{-3} M) by standard curve-fitting[17] of a chemical shift vs concentration plot and has been estimated at 830 M^{-1}. At higher concentration, the shape of this curve is very complex due to superimposition of multiple aggregation equilibriums up to final precipitation.

Electrospray Mass Spectrometry. Experimental investigations in electrospray mass spectrometry carried out on the dinuclear complex **1** are also consistent with this aggregation hypothesis. The recent electrospray mass spectrometry technique (ESMS) which belongs to the class of soft ionization methods[18] appears as a powerful tool for characterizing noncovalent architectures. As a matter of fact, numerous complex systems involving noncovalent interactions (host−guest species,[19] hydrogen-bonded supramolecular assemblies,[20] enzyme−substrate associations,[21] heme−protein complexes,[22] oligonucleotide duplexes,[23] formation of multinuclear metal coordination complexes under equilibrium conditions[24]) have been successfully evidenced on using this low-energy technique which does not perturb weak interactions.

The mass spectra showed the four pseudomolecular peaks at *m*/*z* (state of charge): 1783 (1+), 864 (2+), 526 (3+), 359.9 (4+) characterizing the neutral bqpy complex **1** after loss of respectively one, two, three, and four PF_6^- counteranions. A fifth peak was also found at $m/z = 1200$ and its *m*/*z* value as well its 3+ state of charge suggested the formation of the dimeric ion $\{[(bpy)_2Ru(bqpy)Ru(bpy)_2]_2\}(PF_6^-)_5\}^{3+}$. An accurate isotopic resolution of the higher *m*/*z* peak has actually shown the overlap of two species, one being the 1+ charged dinuclear complex and the other being the 2+ charged supramolecular dimeric complex. As the cone voltage was raised to 90 V and then 120 V, the peak intensities relative to the dimer diminished and eventually disappeared while the monomer peak distribution was not affected at all. We observed the simultaneous appearance of a novel peak at $m/z = 1140$ with a state of charge 2^+ corresponding to the $[(bpy)_2Ru(bqpy)]^{2+}$ ion coming from the fragmentation of the dinuclear complex at higher voltage energy.

Molecular Orbital Calculations. Extended Hückel calculations[12] were performed on the free bqpy ligand (Figure 2). Comparison with the tpphz orbital scheme emphasizes their similar electronic distribution and allows a good understanding of their close electrochemical and photophysical properties. For both ligands, we made the following observations:

(i) the two lowest vacant molecular orbitals are centered on the central part with a phenazine-like electronic distribution without any significant weight on the coordinating outer nitrogens. These LUMO and LUMO+1 are found at −10.36 and −10.31 eV, respectively, and are not stabilized compared to tpphz (−10.35 eV) despite the extension of the aromatic part. Actually it has been observed[25] that angular annelation destabilizes linearly annelated polyaromatic systems. For instance, benzo[*a*]phenazine and dibenzo[*a*,*h*]phenazine are reduced at a more negative potential by 90 and 160 mV, respectively, compared to phenazine. Extended Hückel calculations on the analogous tetrapyridotetraazahexacene, with the same linear polyacene skeleton as bqpy but without the two orthogonally fused benzene (the pyrene core), showed that it had a similar but much more stabilized LUMO (−11.0 eV) which leads to a smaller HOMO−LUMO gap (0.46 vs 1.14 eV in bqpy).

(ii) In contrast, as already noticed in the case of the LUMO+1 of tpphz (Figure 2), the next two degenerated vacant MOs LUMO+2 and LUMO+3 lying at higher energy are developed on the bipyridine-type extremities with a strong weight on the

(17) (a) Horman, I.; Dreux, B. *Helv. Chim. Acta* **1984**, *67*, 754 (b) Marcus, S. H.; Miller, S. I. *J. Am. Chem. Soc.* **1966**, *88*, 3719. (c) Saunders: M.; Hyne, J. B. *J. Chem. Phys.* **1958**, *29*, 1319. (d) Shetty, A. S.; Zhang, J.; Moore, J. S.*J. Am. Chem. Soc.* **1996**, *118*, 1019 and references therein.
(18) M. Przybylski and M. O. Glocker, *Angew. Chem., Int. Ed. Engl.* **1996**, *35*, 806 and references therein.
(19) Ganem, B.; Li, Y.-T.; Henion, J. D. *J. Am. Chem. Soc.* **1991**, *113*, 6294.
(20) (a) Russel, K. C. Leize, E.; Van Dorsselaer, A.; Lehn, J.-M. *Angew. Chem., Int. Ed. Engl.* **1995**, *34*, 209. (b) Ma, S.; Rudkevich, D. M.; Rebek, J. *J. Am. Chem. Soc.* **1998**, *120*, 4977.
(21) (a) Baca, M.; Kent, S. B. *J. Am. Chem. Soc.* **1992**, *114*, 3992. (b) Ganem, B.; Li, Y.-T.; Henion, J. D. *J. Am. Chem. Soc.* **1991**, *113*, 7818.
(22) Katta, V.; Chait, B. T. *J. Am. Chem. Soc.* **1991**, *113*, 8534.
(23) Ganem, B.; Li, Y.-T.; Henion, J. D. *Tetrahedron Lett.* **1993**, *34*, 1445.
(24) (a) Leize, E.; Van Dorsselaer, A.; Krämer, R.; Lehn, J.-M. *J. Chem. Soc. Chem. Commun.* **1993**, 990. (b) Marquis-Rigault, A.; Dupont-Gervais, A.; Baxter, P. N. W.; Van Dorsselaer, A.; Lehn, J.-M. *Inorg. Chem.* **1996**, *35*, 2307 and references therein. (c) Marquis-Rigault, A.; Dupont-Gervais, A.; Van Dorsselaer; A.; Lehn, J.-M. *Chem. Eur. J.* **1996**, *2*, 1395. (d) Hasenknopf, B.; Lehn, J.-M.; Boumediene, N.; Dupont-Gervais, A.; Van Dorsselaer, A.; Kneisel, B.; Fenske, D. *J. Am. Chem. Soc.* **1997**, *119*, 10956. (e) Russel, K. C.; Leize, E.; Van Dorsselaer, A.; Lehn, J.-M. *Angew. Chem.* **1995**, *107*, 244; *Angew. Chem., Int. Ed. Engl.* **1995**, *34*, 209.
(25) Modler-Spreitzer, A.; Mannschreck, A.; Schotz, M.; Gescheidt, G.; Spreitzer, H.; Daub, J. *J. Chem. Research (M)* **1995**, 1229.

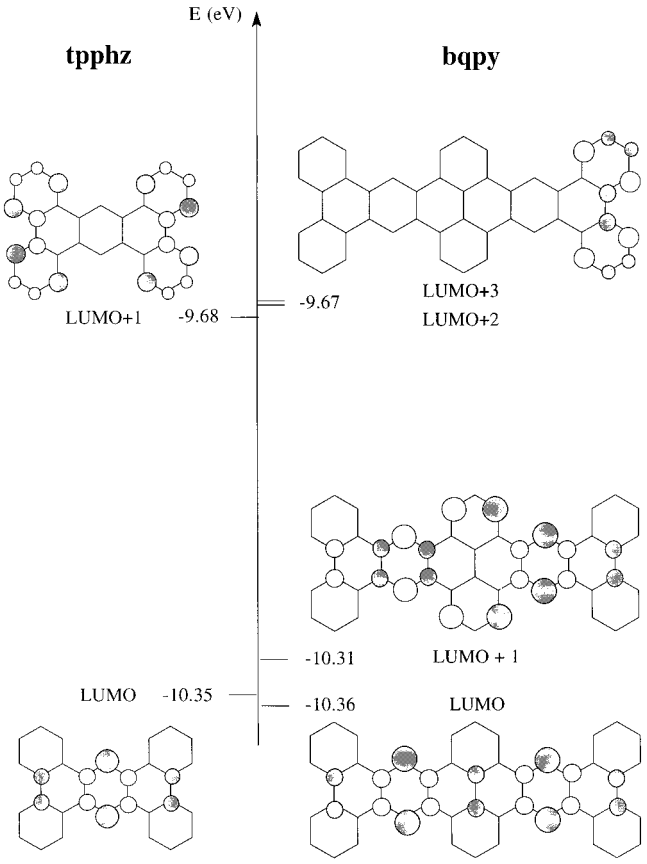

Figure 2. Electronic structures of tpphz and bqpy. The LUMO+2 and LUMO+3 are degenerate. Only one is shown here, the second being symmetrical with respect to the center of the molecule.

coordinating nitrogens and no more electronic density on the phenazine-type nitrogens and the ligand central part.

This simple electronic approach indicates that the bqpy core can be considered as mainly composed of two fused pyrazine-like motifs without any significant orbital overlap with the bipyridine-like ends. This electronic distribution and the orbital energy levels account also for the more pronounced π-attractor character and the greater energetic stabilization of bqpy and tpphz with respect to those of the bipyridine ligand.

Extension of the calculations toward the dinuclear complex itself was precluded by the program limitations concerning the number of atoms. However, previous studies on the quinoxalinic tpphz[3] and dppz[26] complexes have established that only the HOMOs were metal localized and that no real change of the LUMO energies and compositions occurred while going from the free ligand to its complexed form. The higher unoccupied MOs were essentially spread either on the ancillary bipyridines or on the bipyridine-type tpphz ends whereas the HOMOs were metal localized. The very similar vacant MOs of the free bqpy and tpphz and, in both cases, their coordination to $[Ru(bpy)_2]^{2+}$ -type extremities allow us to extend the results obtained on the ligand to the bqpy complex. The electrochemical characterizations described below will actually valid such an assumption.

Electrochemistry. Cyclic voltammograms of **1** (CH_3CN or DMF/0.1 M $^nBu_4NPF_6$, Table 1) in the -2.3 to 1.5 V potential window (vs SCE) and showed six successive quasi-reversible waves attributed to one metal-centered oxidation and five ligand-based reductions (Scheme 2).

(26) (a) Chambron, J.-C.; Sauvage, J.-P.; Amouyal, E.; Koffi, P. *Nouv. J. Chim.* **1985**, *9*, 527. (b) Fees, J.; Kaim, W.; Moscherosch, M.; Matheis, W.; Klima, J.; Krjcicik, M.; Zalis, S. *Inorg. Chem.* **1993**, *32*, 166.

The oxidation part of the bqpy dinuclear complex exhibited one two-electron single wave at $E_{1/2} = 1.35$ V (vs SCE) for both $Ru^{II}-Ru^{III}$ redox couples. This superimposition confirms that the long intermetallic distance (ca. 20 Å) precludes any important Coulombic interaction between these remote metallic centers. As observed for the tpphz dinuclear and tetranuclear complexes,[3a] this oxidation half-wave potential is very close to that of $[(Ru(bpy)_3]^{2+}$ despite the very strong π-withdrawing character of the quinoxalinic ligands. This is consistent with a small contribution from the phenazine part to the HOMO with an orbital scheme very similar to that of $[(Ru(bpy)_3]^{2+}$.

The first two reduction processes occur at a potential of -0.9 and -1.07 V respectively and involve each one electron. In contrast with oxidation, the reduction values are significantly anodically shifted with respect to those of $[Ru(bpy)_3]^{2+}$ which stresses the better π-electron acceptor character of the bqpy containing complex. This is consistent with the addition of one electron on each of the two low-energy LUMO and LUMO+1 mainly localized on the phenazine part of bqpy to give the complexes $[(bpy)_2Ru(\mathbf{bqpy})^{\bullet-}Ru(bpy)_2]^{3+}$ and $[(bpy)_2Ru(\mathbf{bqpy})^{2-}$-$Ru(bpy)_2]^{2+}$. The proximity of these two reduction processes stresses that the added electrons in the LUMO and LUMO are occupying nonoverlapping parts of the central core with small Coulombic repulsions.

The third and fourth reduction waves (-1.31 and -1.52 V) appear at almost the same potentials as the first and second reductions of $[Ru(bpy)_3]^{2+}$ (respectively -1.31 and -1.50 V) and involve two electrons each. These processes are attributed to the simultaneous reductions of one ancillary bipyridine at each metallic extremity to give first the species $[\{(bpy)(\mathbf{bpy}^{\bullet-})$-$Ru(bqpy)^{2-}Ru(\mathbf{bpy}^{\bullet-})(bpy)]$ and then $[\{(\mathbf{bpy}^{\bullet-})(bpy^{\bullet-})Ru(bqpy)^{2-}$-$Ru(bpy^{\bullet-})(\mathbf{bpy}^{\bullet-})]^{2-}$ and are not affected by the presence of two electrons on the bqpy part. This extensive decoupling between the bridging and the ancillary ligands was already observed for the tpphz complexes,[3a] and is a clear indication of the lack of any significant molecular orbital overlap between the unoccupied bpy-like MOs developed on the coordinated nitrogens and the other lowest MO developed on the central quinoxalinic nitrogens. So not only the oxidation but also the reduction potential values agree with a ruthenium electronic surrounding very similar to that of a $[Ru(bpy)_3]^{2+}$ moiety uncoupled to the central part of the bridging ligand. Finally the fifth wave appears at -1.86 V and involves two electrons. Its larger width ($E_{pa} - E_{pc}$ *ca.* 250 mV) suggests the superimposition of two very close monoelectronic processes, attributed to the further reduction of the bqpy ligand by analogy with the tpphz mononuclear complexes.

Absorption Spectra. The absorption spectrum of **1** is reported in Figure 3 and compared with those of related mononuclear and binuclear complexes $[(bpy)_2Ru(tpphz)]^{2+}$ and $[(bpy)_2Ru(tpphz)Ru(bpy)_2]^{4+}$. It comprises three distinct regions as usually observed for polypyridyl complexes. The first region at $\lambda < 320$ nm is composed of intense $\pi-\pi^*$ bpy centered transitions while the second region shows two sharp bands at 335 and 420 nm assigned to $\pi-\pi^*$ bqpy centered transitions. The red shift observed in going from the tpphz complex to the bqpy one is as expected on the basis of a larger delocalization within the more extended bridge. The 420-nm band is superimposed on a broader band system peaking at ca. 450 nm, and containing the typical MLCT transitions of Ru(II) polypyridine complexes $Ru^{II} \rightarrow bpy(\pi^*)$ and $Ru^{II} \rightarrow bqpy(\pi^*)$. The molar absorptivities in this spectral region scale approximately as the total number of MLCT transitions expected for the nuclearity (two) of the dinuclear complex. From Figure 3, it can be seen

Table 1. Half-Wave Potentials E (Volts) for the Oxidation E_{OX} and the Reduction E_{red} of the Complexes[a,b]

species	E_{ox}	E_{red1}	E_{red2}	E_{red3}	E_{red4}	E_{red5}
$[Ru(bpy)_3]^{2+}$ [c]	1.27	−1.31	−1.50	−1.77		
$[Ru(bpy)_2(bqpy)Ru(bpy)_2]^{4+}$	1.35 (2 e$^-$)	−0.90 (1 e$^-$)	−1.07 (1 e$^-$)	−1.31(2 e$^-$)	−1.52 (2 e$^-$)	−1.86 (2 e$^-$)
$[Ru(bpy)_2(tpphz)]^{2+}$ [d]	1.33	−0.87	−1.33	−1.51	−1.83	
$[Ru(bpy)_2(tpphz)Ru(bpy)_2]^{4+}$ [d]	1.34 (2 e$^-$)	−0.71 (1 e$^-$)	−1.31 (2 e$^-$)	−1.51 (2 e$^-$)	−1.72 (1 e$^-$)	

[a] Unless otherwise noted the oxidation potentials are given vs SCE in CH_3CN and the reduction potentials are given vs SCE in DMF; in both cases the supporting electrolyte is 0.1 M nBu_4NPF_6 at room temperature; scan speed 0.1 V s^{-1}; internal reference $Fc/Fc^+ = 0.48$ V. [b] All complexes are PF_6 salts. [c] From ref 27, in acetonitrile. [d] From ref 3a.

Scheme 2. Electrochemical Processes of **1** in the Range 1.5 to −2.3 V vs SCE

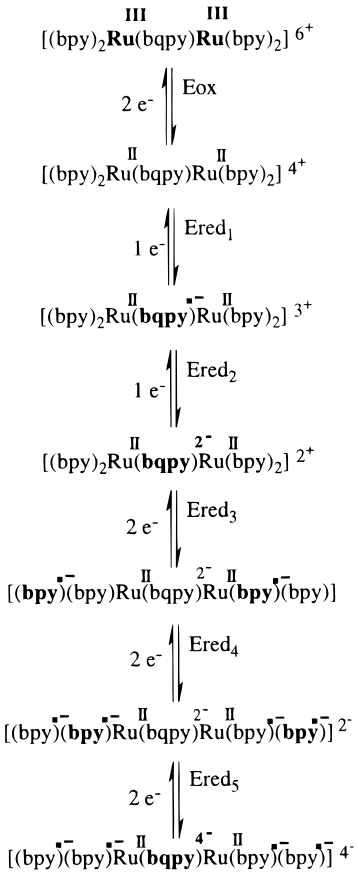

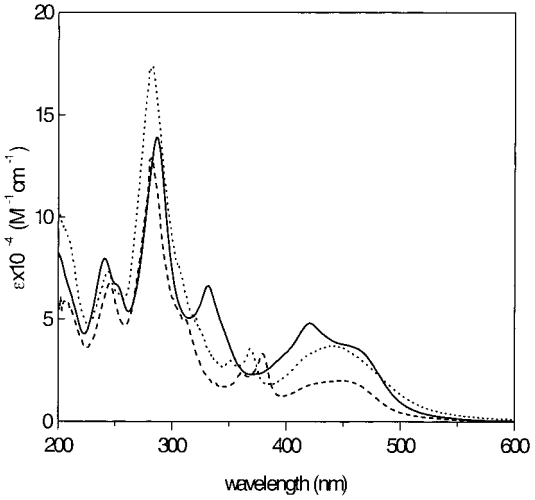

Figure 3. Absorption spectra in acetonitrile solution of **1** (—), and of the model compounds $[(bpy)_2Ru(tpphz)]^{2+}$ (- -) and $[(bpy)_2Ru(tpphz)Ru(bpy)_2]^{4+}$ (...).

Table 2. Photophysical Properties of $[(bpy)_2Ru(bqpy)Ru(bpy)_2]^{4+}$ and Related Complexes; Emission Maxima Are Corrected for the PMT Response.

	RT			77 K	
complexes	λ_{max} (nm)	τ (ns)[a]	Φ_{em} ($\times 10^2$)	λ_{max} (nm)[b]	τ (ns)[b]
$[Ru(bpy)_3]^{2+}$	620	1100	6	580	5100
$[(bpy)_2Ru(tpphz)]^{2+}$	628	1090	4.5	580	4000
$[(bpy)_2Ru(tpphz)Ru(bpy)2]^{4+}$	740	90	0.084	585	2800
$[(bpy)_2Ru(bqpy)Ru(bpy)_2]^{4+}$	628	1080	5.0	581	3200

[a] CH_3CN, deaerated solutions. [b] Rigid matrix, EtOH/MetOH 4/1.

that this MLCT band is very similar to those of $[(bpy)_2Ru(tpphz)]^{2+}$ and $[(bpy)_2Ru(tpphz)Ru(bpy)_2]^{4+}$.[28] This band is not red-shifted as might have been expected with a longer polyaromatic ligand, and the absorption wavelengths are also very close to that of the $[Ru(bpy)_3]^{2+}$ despite the good π-accepting character of bqpy. Actually, the lowest energy MLCT bands related to HOMO→LUMO and LUMO+1 are probably very weak. As indicated by EH calculations, these two LUMO are mainly localized on the central part of bqpy, with very small coefficients on the bqpy phenanthroline nitrogen atoms, which induces small extinction coefficients through small oscillator strength.[29] These weak absorptions are overlapped by the intense HOMO to LUMO+2 and HOMO to LUMO+3 bands involving two unoccupied orbitals with large coefficients on the phenanthroline part of bqpy and on the ancillary bpy, and with a MO composition similar to that found in $[Ru(bpy)_3]^{2+}$.

Photophysics of $[(bpy)_2Ru(bqpy)Ru(bpy)_2]^{4+}$. The photophysical properties of $[(bpy)_2Ru(bqpy)Ru(bpy)_2]^{4+}$ can be compared with those of the mononuclear and binuclear complexes $[Ru(bpy)_3]^{2+}$, $[(bpy)_2Ru(tpphz)]^{2+}$, and $[(bpy)_2Ru(tpphz)Ru(bpy)_2]^{4+}$. The results of the full photophysical characterization of $[(bpy)_2Ru(bqpy)Ru(bpy)_2]^{4+}$ are summarized in Table 2.

The emission of the binuclear $[(bpy)_2Ru(bqpy)Ru(bpy)_2]^{4+}$ complex (as those of the model compounds), both at room temperature and at 77 K, appears to be, from all experimental evidence, a single MLCT emission as (i) the excitation spectrum closely matches the absorption spectrum and (ii) the emission decays with constant profile and single-exponential kinetics. It is interesting to notice that the emission energy, lifetime, and quantum yield of the binuclear complex $[(bpy)_2Ru(bqpy)Ru(bpy)_2]^{4+}$ are quite different from those of the binuclear complex $[(bpy)_2Ru(tpphz)Ru(bpy)_2]^{4+}$, but very similar to those of the mononuclear complex $[(bpy)_2Ru(tpphz)]^{2+}$ (Table 2). In the case

(27) Rillema, D. P.; Allen, G.; Meyer, T. J.; Conrad, D. *Inorg. Chem.* **1983**, *22*, 1617.

(28) Actually, $[(bpy)_2Ru(tpphz)Ru(bpy)_2]^{4+}$ featured a small increase in absorption in the long-wavelength edge of the MLCT band system ($\lambda_{max} \cong 500$ nm), relative to $[(bpy)_2Ru(tpphz)]^{2+}$. Apparently, $[(bpy)_2Ru(bqpy)Ru(bpy)_2]^{4+}$ does not even show this feature.

(29) (a) Ernst, S. D.; Kaim, W. *J. Am. Chem. Soc.* **1986**, *108*, 3578. (b) Ernst, S. D.; Kaim, W. *Inorg. Chem.* **1989**, *28*, 1520.

of $[(bpy)_2Ru(tpphz)Ru(bpy)_2]^{4+}$,[30] the red shift in emission relative to $[(bpy)_2Ru(tpphz)]^{2+}$ (with the consequent changes in photophysical properties) was the effect of increased π^* delocalization upon binding of the second metal, a common feature of systems involving conjugated bridging ligands.[31] Evidently, the bqpy ligand does not show this feature despite its length.

In electrochemistry, similar behaviors have been observed as the first reduction potential (corresponding to reduction of the bridging ligand) of $[(bpy)_2Ru(bqpy)Ru(bpy)_2]^{4+}$ is practically coincident with that of the mononuclear complex $[(bpy)_2Ru(tpphz)]^{2+}$ (-0.87 V) but largely differs from that of the dinuclear complex $[(bpy)_2Ru(tpphz)Ru(bpy)_2]^{4+}$ (-0.71 V).

To sum up, both the photophysical and electrochemical data are in agreement with the molecular orbital scheme, supporting the picture of a $[(bpy)_2Ru(bqpy)Ru(bpy)_2]^{4+}$ dinuclear complex composed of two practically independent halves, each moiety being similar to the mononuclear $[(bpy)_2Ru(tpphz)]^{2+}$ species, the pyrene part being an "insulator" between the π systems of the two halves of the ligand.

Conclusion

The dinuclear ruthenium complex $\{(bpy)_2Ru(bqpy)Ru(bpy)_2]^{4+}$ (**1**), with a Ru−Ru distance of 20 Å, can be prepared by a stepwise condensation of a diamino ruthenium complex and tetraketopyrene. The presence of the long polyaromatic bqpy ligand allows the aggregation of these dinuclear complex in solution to give the dimer $[\mathbf{1}_2]^{8+}$ stable enough to be observed by electrospray mass spectrometry. The existence of well-distinct and nonoverlapping electronic regions despite the large and fully conjugated character of the bridging ligand has been clearly established from electrochemical and spectroscopic measurements and accounts for the lack of efficient metal−metal electronic coupling. The presence of two angularly fused aromatic cycles on the polyacene chain seems to be at the origin of the formation of uncoupled electronic loops. The study this electronic effect on the metal−metal coupling in polyacene and polyrylene systems is currently under investigation.

Acknowledgment. The financial assistance of CNRS (France), MURST and CNR (Italy), and EEC (HCM Network CHRXCT-94-0538) is gratefully acknowledged. Thanks are also expressed to G. Balacco (Menarini Industrie) for a copy of SwaN-MR, to J. C. Cobas, J. Cruces, and F. Sardina for a copy of MestRe-C, to S. Richelme and C. Claparols for ESMS experiments, and to C. Viala (CEMES) for NMR experiments.

Supporting Information Available: Preparation and characterization of **5** and emission spectra of **1**. This material is available free of charge via the Internet at http://pubs.acs.org.

IC9812196

(30) Chiorboli, C.; Bignozzi, C. A.; Scandola, F.; Ishow, E.; Gourdon, A.; Launay, J.-P., in preparation.

(31) (a) Hammarstrom, L.; Barigelletti, F.; Flamigni, L.; Indelli, M. T.; Armaroli, N.; Calogero, G..; Guardigli, M.; Sour, A.; Collin, J. P.; Sauvage, J. P. *J. Phys. Chem* **1997**, *101*, 9061. (b) Grosshenny, V.; Harriman, A.; Ziessel, R. *Angew. Chem., Int. Ed. Engl.* **1995**, *34*, 2705.